



TITLE:

Dynamic Transport and Cementation of Skeletal Elements Build Up the Pole-and-Beam Structured Skeleton of Sponges.

AUTHOR(S):

Nakayama, Sohei; Arima, Kazushi; Kawai, Kotoe; Mohri, Kurato; Inui, Chihiro; Sugano, Wakana; Koba, Hibiki; ... Fujimori, Toshihiko; Agata, Kiyokazu; Funayama, Noriko

CITATION:

Nakayama, Sohei ...[et al]. Dynamic Transport and Cementation of Skeletal Elements Build Up the Pole-and-Beam Structured Skeleton of Sponges.. Current biology : CB 2015, 25(19): 2549-2554

ISSUE DATE:

2015-10-05

URL:

<http://hdl.handle.net/2433/201533>

RIGHT:

© 2015. This manuscript version is made available under the CC-BY-NC-ND 4.0 license <http://creativecommons.org/licenses/by-nc-nd/4.0/>; The full-text file will be made open to the public on 5 October 2016 in accordance with publisher's 'Terms and Conditions for Self-Archiving'; This is not the published version. Please cite only the published version.; この論文は出版社版ではありません。引用の際には出版社版をご確認ご利用ください。

Dynamic Transport and Cementation of Skeletal Elements Build Up the Pole-and-Beam Structured Skeleton of Sponges

Sohei Nakayama,^{1,5,6} Kazushi Arima,^{1,5,7} Kotoe Kawai,¹ Kurato Mohri,^{1,8} Chihiro Inui,¹ Wakana Sugano,¹ Hibiki Koba,¹ Kentaro Tamada,¹ Yudai J. Nakata,¹ Kouji Kishimoto,¹ Miyuki Arai-Shindo,¹ Chiaki Kojima,¹ Takeo Matsumoto,² Toshihiko Fujimori,³ Kiyokazu Agata,¹ and Noriko Funayama^{1,4*}

¹Department of Biophysics, Graduate School of Science, Kyoto University, Kitashirakawa-oiwake, Sakyo-ku, Kyoto 606-8502, Japan

²Department of Mechanical Engineering, Graduate School of Engineering, Nagoya Institute of Technology, Gokiso-cho, Showa-ku, Nagoya, Aichi 466-8555, Japan

³Division of Embryology, National Institute of Basic Biology, 5-1 Higashiyama, Myodaiji, Okazaki, Aichi 444-8787, Japan

⁴Precursory Research for Embryonic Science and Technology (PRESTO) Program, Japan Science and Technology Agency (JST), 4-1-8 Honcho, Kawaguchi, Saitama 332-0012, Japan

⁵Co-first author

⁶Present address: Multicellular Organization Laboratory, National Institute of Genetics, Yata 1111, Mishima, Shizuoka 411-8540, Japan

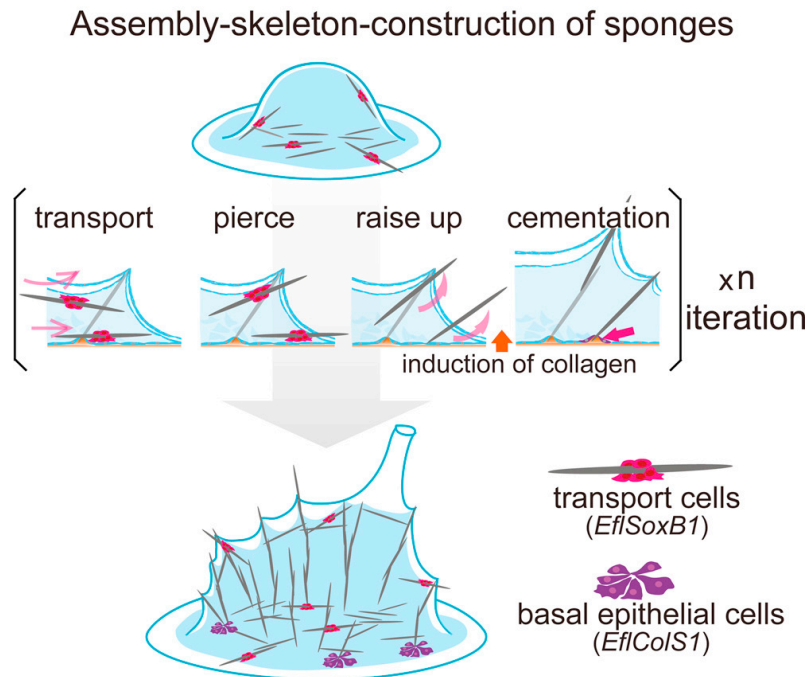
⁷Present address: Faculty of Medicine, Tottori University, 86 Nishi-cho, Yonago, Tottori 683-8503, Japan

⁸Present address: Department of Bioinformatics, College of Life Sciences, Ritsumeikan University, Noji-higashi 1-1-1, Kusatsu, Shiga 525-8577, Japan

*Correspondence: funayama@mdb.biophys.kyoto-u.ac.jp

<http://dx.doi.org/10.1016/j.cub.2015.08.023>

Graphical Abstract



In Brief

Nakayama et al. find that the inner body skeleton of sponges is constructed by mechanisms fundamentally different from the known skeleton formation of animals. The spicules are dynamically transported by newly discovered “transport cells,” and the iteration of sequential mechanical reactions of player cells builds up sponges’ skeletons spicule by spicule.

Highlights

- Live imaging shows dynamic transport and assembly of spicules in *E. fluviatilis*
- Newly discovered “transport cells” carry and finally push spicules through epithelia
- Raised-up spicules are cemented by collagen expressed in basal epithelial cells
- Iteration of “transport-pierce-raise up-cementation” constructs the skeleton

SUMMARY

Animal bodies are shaped by skeletons, which are built inside the body by biomineralization of condensed mesenchymal cells in vertebrates [1, 2] and echinoderms [3, 4], or outside the body by apical secretion of extracellular matrices by epidermal cell layers in arthropods [5]. In each case, the skeletons' shapes are a direct reflection of the pattern of skeleton-producing cells [6]. Here we report a newly discovered mode of skeleton formation: assembly of sponges' mineralized skeletal elements (spicules) in locations distant from where they were produced. Although it was known that internal skeletons of sponges consist of spicules assembled into large pole-and-beam structures with a variety of morphologies [7-10], the spicule assembly process (i.e., how spicules become held up and connected basically in staggered tandem) and what types of cells act in this process remained unexplored. Here we found that mature spicules are dynamically transported from where they were produced and then pierce through outer epithelia, and their basal ends become fixed to substrate or connected with such fixed spicules. Newly discovered "transport cells" mediate spicule movement and the "pierce" step, and collagen-secreting basal-epithelial cells fix spicules to the substratum, suggesting that the processes of spiculous skeleton construction are mediated separately by specialized cells. Division of labor by manufacturer, transporter, and cementer cells, and iteration of the sequential mechanical reactions of "transport," "pierce," "raise up," and "cementation," allows construction of the spiculous skeleton spicule by spicule as a self-organized biological structure, with the great plasticity in size and shape required for indeterminate growth, and generating the great morphological diversity of individual sponges.

RESULTS

Sponges have unique internal body skeletons composed of fine spicules connected into pole-and-beam structures in a manner similar to architectural construction [7-10]. Siliceous spicules are produced intracellularly in sclerocytes [11-14] and are thought to be released when they mature (Figure 1A). Spicules are fixed to the substrate by embedding in thickened collagenous matrix under the basal epithelium (basopinacoderm) or are coated and connected by collagenous matrix, according to electron microscopic studies in demosponges (which constitute more than 90% of sponge species, including

Ephydatia) [8, 15]. How spicules are assembled has remained a mystery, mainly because of the lack of studies at the cellular and spicule levels.

To investigate skeleton construction of demosponges from the earliest phase, we are focusing on gemmule hatching, a form of asexual reproduction in the freshwater demosponge *Ephydatia fluviatilis* whereby a functional miniature sponge develops from a group of totipotent stem cells packed inside a gemmule [16] (Figure 1B). Our previous work using a sclerocyte lineage marker we identified, *EflSilicateinM1*, showed that spicule production could be detected in sclerocytes scattered in the sponge body around stage 2 and continues thereafter (Figure 1B) [12, 13].

Spicules Are Dynamically Moved and Then Become Held Up

By obtaining side-view images of juvenile sponges captured by placing a mirror in a microscope's light path, we clearly showed that spicule holding-up starts around stage 2.5, and that skeleton construction continues along with sponge growth (Figure 1C).

For live imaging, we labeled spicules via incorporation of a fluorescent dye from the culture medium during spicule production, inspired by diatom studies [17]. From time-lapse movies of the side-view images, we found that spicules are held up one by one from an almost flat position (Figure 1D). Time-lapse images of the planar view revealed that mature-sized spicules (>150 μm in our experimental conditions [13]) traveled dynamically, even as far as the opposite side of the sponge body (>1 mm; Figure 1E), and then those moved spicules became held up (Figures 1E and 1F; Movie S1) roughly in a circle (here designated a “circular row”). Note that more spicules became held up according to the growth of sponges, basically outside the circular row but not in a concentric manner (data not shown). The trajectories of the held-up spicules showed that spicules moved in the direction of their long axis, both forward and backward, and rather stochastically, except for their tendency to move toward the periphery of the sponge body, a tendency also shown by other cells in the mesohyl (inner body space) (Figures 1E and 1G). The spicule holding-up points (SHU points) in the circular row often showed similar spacing to each other in some parts of the body but were also often more randomly located (Figures 1E and 1G). Despite intense analysis of more than 200 trajectories of spicule movements such as those shown in Figure 1G and Movie S2, we could not find any obvious routes of spicule movement or rules about the distance between moving spicules. Furthermore, we could not find any rules about the order in which spicules are held up (such as “after a first spicule is held up, spicules are held up in

the farthest positions from the already held-up spicules, or at a certain distance from them”). These data clarified that spicules are transported before becoming held up, and thus where spicules become held up is distinct from where they were produced. Additionally, spicules appeared to become held up independently of each other, and it seemed unlikely that there was pre-patterning of where spicules should be held up.

A Specific Type of Cells, Designated “Transport Cells,” Mediates Spicule Movement

What, then, drove the movement of spicules? In bright-field time-lapse movies, we found that moving spicules, but not immobile spicules, had cells attached to their midpoint or slightly in front of it (Figure 2A; Movie S3). The dynamically changing morphology of the attached cell (or cells) suggested that they might mediate spicule transport (Movie S3). One candidate for these possible spicule-carrying cells was sclerocytes, which might move to where spicules would become held up and release the mature spicules there. Alternatively, one or more other types of cells might be involved. Until now, spicule-carrying cells have not been reported, although Norbert Weissenfels predicted them [15]. Serendipitously, we found that *EflSoxBI* mRNA is expressed specifically in the group of cells attached near the middle of moving spicules, contrary to its expected expression in archeocytes (stem cells). Since introduction of genes to sponge cells has not yet succeeded, we instead performed combinatory time-lapse recording followed by whole-mount in situ hybridization (TLR-WISH) and thereby confirmed that *EflSoxBI*-expressing cells were attached to all of the mature-sized spicules that moved, but not to any immobile spicules (Figures 2B and 2C, magenta arrowheads and blue arrowheads, respectively). Fluorescent detection of WISH showed that multiple cells are attached around the middle of spicules (Figure 2D). The *EflSoxBI*-expressing cells attached to the spicules were clearly different from spicule-containing sclerocytes (expressing marker gene *EflSlicateinMI*) (Figures 2E and S1). Based on these data, we concluded that *EflSoxBI*-expressing cells are possible spicule-carrying cells and thus designated them “transport cells.”

Transport Cells Push a Carried Spicule through Outer Epithelia to Initiate Raising Up of the Pierced End of the Spicule

We then asked how spicules become held up. Time-lapse movies showed that the front ends of carried spicules are eventually raised up, and that even after a spicule’s front end becomes raised up, its basal

end moves for about 2–3 hr and finally becomes immobile (see trajectories in Figures 1E and 1G and Movies S1 and S2). Using confocal microscopy, we found that the front end of a carried spicule just at the edge of the mesohyl seemed to push forward (since the outer epithelia became deformed; Figure 3A, 0 min, 15 min), and finally about half of the spicule protruded through (pierced) the outer epithelia and was slightly raised up (Figure 3A, 30 min; Movie S4). TLR-WISH confirmed the *EflSoxB1*-expression in attached cells when the spicule started to pierce the outer epithelia (Figure 3B; Movie S5). *EflSoxB1*-expressing cells could not be detected on already raised-up spicules (data not shown), suggesting that *EflSoxB1* expression might cease during spicule raising-up, or that transport cells might detach from raised-up spicules. Although further studies will be necessary to unveil the precise mechanisms involved, our results suggested that transport cells not only mediate spicule transport but also act in the unexpected “pierce” step that precedes the “raise up” step (Figure 3C).

Next we addressed whether the collagen matrix in which raised-up spicules are embedded is formed after spicules are raised up, or is preformed. For this, we examined whether mRNA expression of a short-chain collagen, *EflColS1*, occurs after spicules are raised up, or prior to it. We isolated and used *EflColS1* for this purpose because it had been reported that in *Ephydatia muelleri*, a homologous short-chain collagen was expressed in basopinacocytes around held-up spicules, as shown by WISH with rather low resolution using radioisotope-labeled mRNA probe [18, 19]. First, we confirmed that *EflColS1* is expressed in basopinacocytes arranged in rosette shape around the held-up spicules, showing the possible involvement of *EflColS1* in “cementation” of skeletal spicules (Figures 3D and S2). TLR-WISH clarified that *EflColS1* expression was induced after spicules were raised up, and that the number of *EflColS1*-expressing cells was increased (Figure 3E). These data also support the idea that there is no pre-patterning of future SHU points.

Additional Spicules Are Carried on ENCM to Undergo “Transport-Pierce-Raise Up-Cementation” at the Top of a Spicule Forming the Skeleton

We then addressed how additional spicules are carried and connected to the top of the already held-up spicules. Although we had initially hypothesized that additional spicules are carried up along (parallel to) the already held-up spicules, time-lapse videos revealed that additional spicules instead moved on the inner side of the endopinacoderm covering the mesohyl (abbreviated here as ENCM) to the top of the skeleton-constructing spicules (Figure 3F; Movie S6). By the same process as primary-spicule

holding-up (“transport-pierce-raise up-cementation”), additional spicules were connected basically in staggered tandem, and thus the spicule tract was elongated (Figure 3F). It also became clear that transport cells generally transported spicules on epithelium surrounding mesohyl (ENCM+basopinacoderm) (Figure 4). The fact that some primary spicules suddenly appeared to adopt an approximately vertical angle and then become immobile (for example, trajectories 2, 6, and 11 in Figure 1G middle panel; Movie S2) indicates that primary spicules were transported on both basopinacoderm and ENCM from early developmental stages onward.

DISCUSSION

The majority of our knowledge to date about body skeleton construction has been based on vertebrates and arthropods, in which the pattern of where skeleton-producing cells aggregate or become aligned as epithelium is first formed during embryogenesis, and the skeleton is then formed in situ. In this study, we revealed that sponges evolved a conceptually different mode of skeleton construction, i.e., “transport” and “assembly” of spicules. Why did sponges evolve these unique skeleton construction methods? Sponges belong to a group of sessile organisms (including corals and plants) whose growth is plastic (i.e. largely depends on their microenvironment) [20-24] and indeterminate, with great morphological variations among individuals. The process of skeleton construction by spicule assembly we revealed here seemed to comprise the key mechanisms that adjust and link sponges’ skeleton construction to their plastic and indeterminate body growth. The key mechanisms are the division of labor of spicule manufacturers (sclerocytes), transporters (transport cells), and cementers (basopinacocytes and possibly unidentified spicule-coating collagen-expressing cells), and the step of “piercing of the outer epithelia by the carried spicule” (Figure 4). Since the known organization of spicules forming poles of skeletal frameworks in demosponges [10], and even in glass sponges (including *Euplectella* [7, 9]), can be explained by the connection of additional spicules using the “pierce” step revealed in this study, it seems highly possible that the mechanisms we revealed using *Ephydatia* are used generally in sponges. Many precise cellular and molecular mechanisms still remain to be elucidated, such as how transport cells can carry spicules, or how one end of pierced spicules is raised up. Additionally, one of the further questions that need to be answered is how sponges fine-tune

their skeleton construction according to conditions of their microenvironment, such as water flow or stiffness of the substratum, since it is reported that the growth form of marine sponges changes according to the water movement of their environment [20-23].

Intriguingly, our study revealed that the spiculous skeleton of sponges is a self-organized biological structure [25, 26] constructed by collective behaviors of individual cells. A chain of simple and mechanical reactions, “transport-pierce (by transport cells)-raise up (by yet unknown cells and/or mechanisms)-cementation (using collagenous matrix secreted by basopinacocytes and possibly by spicule-coating cells),” adds a spicule to the skeleton, and as a result of the iteration of these sequential behaviors of cells, the spiculous skeleton expands. As far as we know, this is the first report of collective behaviors of individual cells building a self-organized biological structure using non-cellular materials, like the collective behaviors of individual termites building mounds [27, 28]. Thus, our work not only sheds new light on skeleton formation in animals but also might inspire interdisciplinary studies in fields such as theoretical biology [20, 21], bioengineering [7, 9], robotics [28], and architectural engineering, utilizing mechanisms of self-constructing architectures that self-adjust to their environments, including remote environments such as the deep sea or space.

ACCESSION NUMBERS

The accession numbers for *EflSoxB1* and *EflColS1* reported in this paper are Genbank: AB976525 and AB976524, respectively.

SUPPLEMENTAL INFORMATION

Supplemental Information includes two figures, six movies, and Supplemental Experimental Procedures and can be found with this article online at <http://dx.doi.org/10.1016/j.cub.2015.08.023>.

AUTHOR CONTRIBUTIONS

S.N. established, and Y.J.N. and K. Kishimoto improved, the methods of live imaging of spicules. K. Arima gathered the data to identify transport cells. K.M. and K. Kawai performed the analysis of the expression of *EflColSI*. T.M., T.F., and N.F. designed, and H.K., K.T., K. Kawai, and N.F. established, the system to obtain lateral images of sponges. C.I. performed analysis of spicule movements. C.I., W.S., M.A.-S., and C.K. provided technical support. N.F. supervised the project with advice from K. Agata. N.F. wrote the manuscript.

ACKNOWLEDGMENTS

We are grateful to Dr. Shigeru Kondo and Dr. Hiroyuki Takeda for discussions and to Dr. Elizabeth Nakajima for discussions, intensive reading, and proofreading the English of the manuscript. We thank Dr. Kiyotaka Okada, Dr. Shigeo Hayashi, Dr. Asako Sugimoto, and Dr. Shinya Kuroda for critical reading of the manuscript and suggestions. We also thank Kazuhito V. Tabata, Motoshi Kaya, and Yusuke Maeda for technical advice. This work was supported by Grants-in-Aid for Scientific Research and a Grant-in-Aid for Scientific Research on Innovative Areas from the Ministry of Education, Culture, Sports, Science and Technology (MEXT) of Japan; the Precursory Research for Embryonic Science and Technology (PRESTO) Program of the Japan Science and Technology Agency; and the National Institute for Basic Biology Cooperative Research Program (individual collaborative research projects) to N.F.

REFERENCES

1. Hall, B.K., and Miyake, T. (1995). Divide, accumulate, differentiate: cell condensation in skeletal development revisited. *Int. J. Dev. Biol.* 39, 881–893.
2. Egawa, S., Miura, S., Yokoyama, H., Endo, T., and Tamura, K. (2014). Growth and differentiation of a long bone in limb development, repair and regeneration. *Dev. Growth Differ.* 56, 410–424.
3. Decker, G.L., and Lennarz, W.J. (1988). Skeletogenesis in the sea urchin embryo. *Development* 103, 231–247.
4. Adomako-Ankomah, A., and Etensohn, C.A. (2013). Growth factor-mediated mesodermal cell guidance and skeletogenesis during sea urchin gastrulation. *Development* 140, 4214–4225.
5. Tajiri, R., Misaki, K., Yonemura, S., and Hayashi, S. (2010). Dynamic shape changes of ECM-producing cells drive morphogenesis of ball-and-socket joints in the fly leg. *Development* 137, 2055–2063.
6. Hall, B.K. (2015). *Bones and Cartilage: Developmental and Evolutionary Skeletal Biology* (Academic Press).
7. Aizenberg, J., Weaver, J.C., Thanawala, M.S., Sundar, V.C., Morse, D.E., and Fratzl, P. (2005). Skeleton of *Euplectella* sp.: structural hierarchy from the nanoscale to the macroscale. *Science* 309, 275–278.
8. Uriz, M.-J. (2006). Mineral skeletogenesis in sponges. *Can. J. Zool.* 84, 322–356.
9. Weaver, J.C., Aizenberg, J., Fantner, G.E., Kisailus, D., Woesz, A., Allen, P., Fields, K., Porter, M.J., Zok, F.W., Hansma, P.K., et al. (2007). Hierarchical assembly of the siliceous skeletal lattice of the hexactinellid sponge *Euplectella aspergillum*. *J. Struct. Biol.* 158, 93–106.
10. Boury-Esnault, N., and Rützler, K. (1997). *Thesaurus of sponge morphology*. *Smithson. Contrib. Zool.* 596, 1–55.
11. Simpson, T.L. (1984). *The Cell Biology of Sponges* (Springer-Verlag).
12. Funayama, N., Nakatsukasa, M., Kuraku, S., Takechi, K., Dohi, M., Iwabe, N., Miyata, T., and Agata, K. (2005). Isolation of Ef silicatein and Ef lectin as molecular markers for sclerocytes and cells involved in innate immunity in the freshwater sponge *Ephydatia fluviatilis*. *Zoolog. Sci.* 22, 1113–1122.

13. Mohri, K., Nakatsukasa, M., Masuda, Y., Agata, K., and Funayama, N. (2008). Toward understanding the morphogenesis of siliceous spicules in freshwater sponge: differential mRNA expression of spicule-type-specific silicatein genes in *Ephydatia fluviatilis*. *Dev. Dyn.* 237, 3024–3039.
14. Ereskovsky, A. (2010). *The Comparative Embryology of Sponges* (Springer).
15. Weissenfels, N. (1978). Bau und Function des Susswasserschwamms *Ephydatia fluviatilis* L. (Porifera). V. Das Nadelskelet und seine Entstehung. *Zool. Jahrb. Anat.* 99, 211–223.
16. Funayama, N. (2013). The stem cell system in demosponges: suggested involvement of two types of cells: archeocytes (active stem cells) and choanocytes (food-entrapping flagellated cells). *Dev. Genes Evol.* 223, 23–38.
17. Li, C.W., Chu, S., and Lee, M. (1989). Characterizing the silica deposition vesicle of diatoms. *Protoplasma* 151, 158–163.
18. Exposito, J.Y., Ouazana, R., and Garrone, R. (1990). Cloning and sequencing of a Porifera partial cDNA coding for a short-chain collagen. *Eur. J. Biochem.* 190, 401–406.
19. Exposito, J.Y., Le Guellec, D., Lu, Q., and Garrone, R. (1991). Short chain collagens in sponges are encoded by a family of closely related genes. *J. Biol. Chem.* 266, 21923–21928.
20. Kaandorp, J.A. (1991). Modeling growth forms of the sponge *Haliclona Oculata* (Porifera, Demospongiae) using fractal techniques. *Mar. Biol.* 110, 203–215.
21. Kaandorp, J.A., and Ku"bler, J.E. (2001). *The Algorithmic Beauty of Seaweeds, Sponges, and Corals* (Springer).
22. Mendola, D., de Caralt, S., Uriz, M.J., van den End, F., Van Leeuwen, J.L., and Wijffels, R.H. (2008). Environmental flow regimes for *Dysidea avara* sponges. *Mar. Biotechnol. (NY)* 10, 622–630.
23. Bosch, T.C., Adamska, M., Augustin, R., Domazet-Loso, T., Foret, S., Fraune, S., Funayama, N., Grasis, J., Hamada, M., Hatta, M., et al. (2014). How do environmental factors influence life cycles and development? An experimental framework for early-diverging metazoans. *BioEssays* 36, 1185–1194.
24. Palmer, C.M., Bush, S.M., and Maloof, J.N. (2012). Phenotypic and developmental plasticity in plants. *eLS*. Published online June 15, 2012. <http://dx.doi.org/10.1002/9780470015902.a0002092.pub2>.
25. Camazine, S., Deneubourg, J.-L., Franks, N.R., Sneyd, J., Theraulaz, G., and Bonabeau, E. (2001). *Self-Organization in Biological Systems* (Princeton University Press).

26. Sasai, Y. (2013). Cytosystems dynamics in self-organization of tissue architecture. *Nature* 493, 318–326.
27. Turner, S.J. (2002). A superorganism's fuzzy boundaries. *Nat. Hist.* 111, 62–67.
28. Werfel, J., Petersen, K., and Nagpal, R. (2014). Designing collective behavior in a termite-inspired robot construction team. *Science* 343, 754–758.

Figure 1.

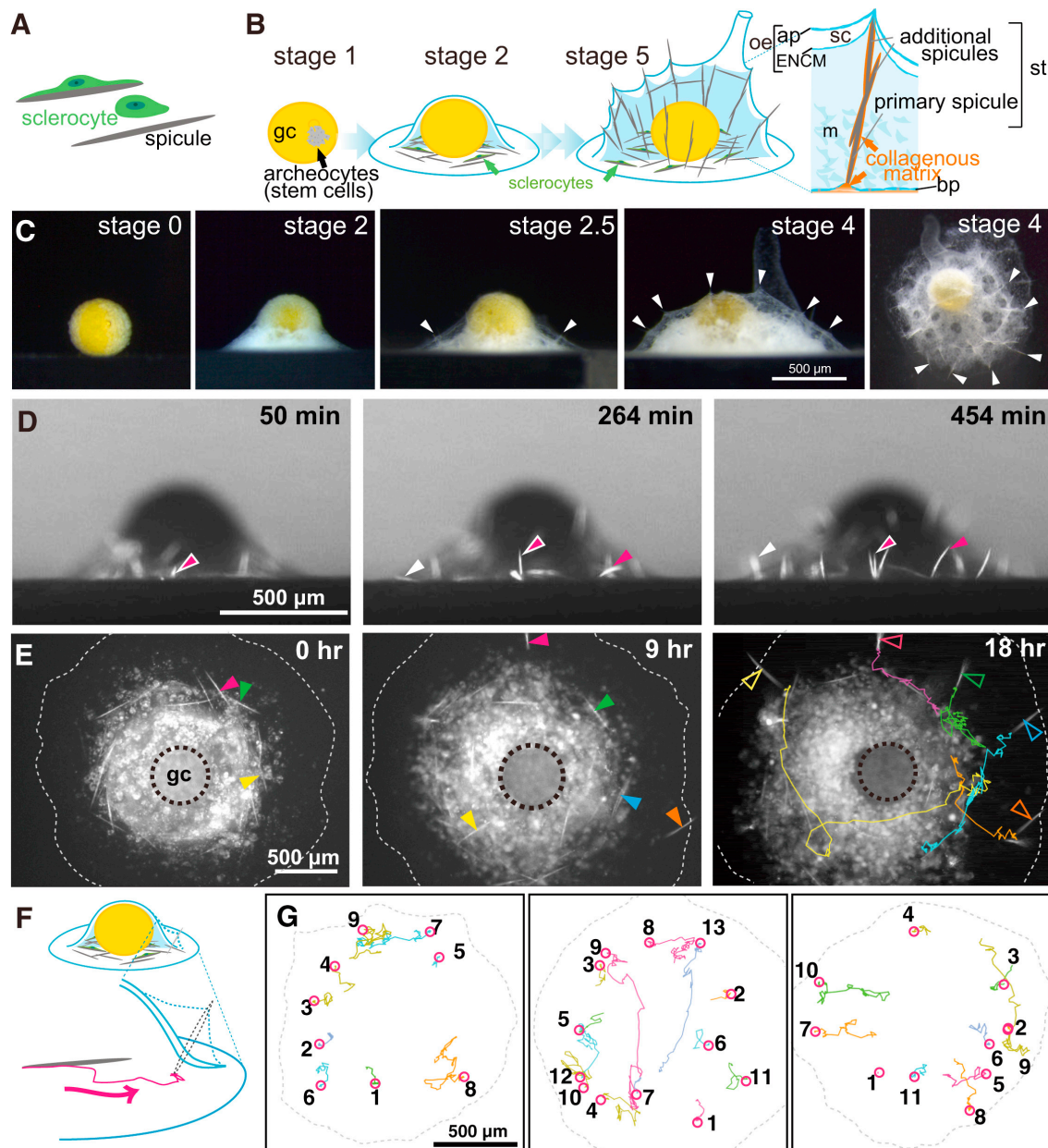


Figure 1. Spicules Are Dynamically Moved and Then Held Up in Sponges

(A) Siliceous spicules are produced intracellularly in sclerocytes. (B) Gemmule hatching of *E. fluviatilis*. ap, apical pinacoderm; bp, basopinacoderm; ENCM, endoderm covering mesohyl; gc, gemmule coat; m, mesohyl; oe, outer epithelia; sc, subdermal cavity; st, spicule tract. Although when and how epithelia of sponges develop has not been clarified, the bodies of juvenile sponges are surrounded by epithelia, and at least by stage 2 we could distinguish ENCM and a subdermal cavity. After spicule tracts (“poles”) elongate, they are connected to other spicule tracts by spicules (“beams”). (C) Views from the side of sponges during gemmule hatching and a view from above (right panel). White arrowheads indicate skeleton-constructing spicules. (D) Captured images of time-lapse video taken from the side of a sponge. Arrowheads indicate primary spicules becoming held up. (E) Time-lapse images obtained from beneath a sponge. Solid arrowheads indicate moving mature-sized spicules. Open arrowheads indicate held-up spicules. See also Movie S1. (F) Illustration showing how a primary spicule moves before becoming held up. (G) Trajectories of the track-back of held-up spicules in z-projected time-lapse movies of three individual sponges are shown by colored lines. Numbered circles indicate order and positions in which spicules were held up. See also Movie S2.

Figure 2.

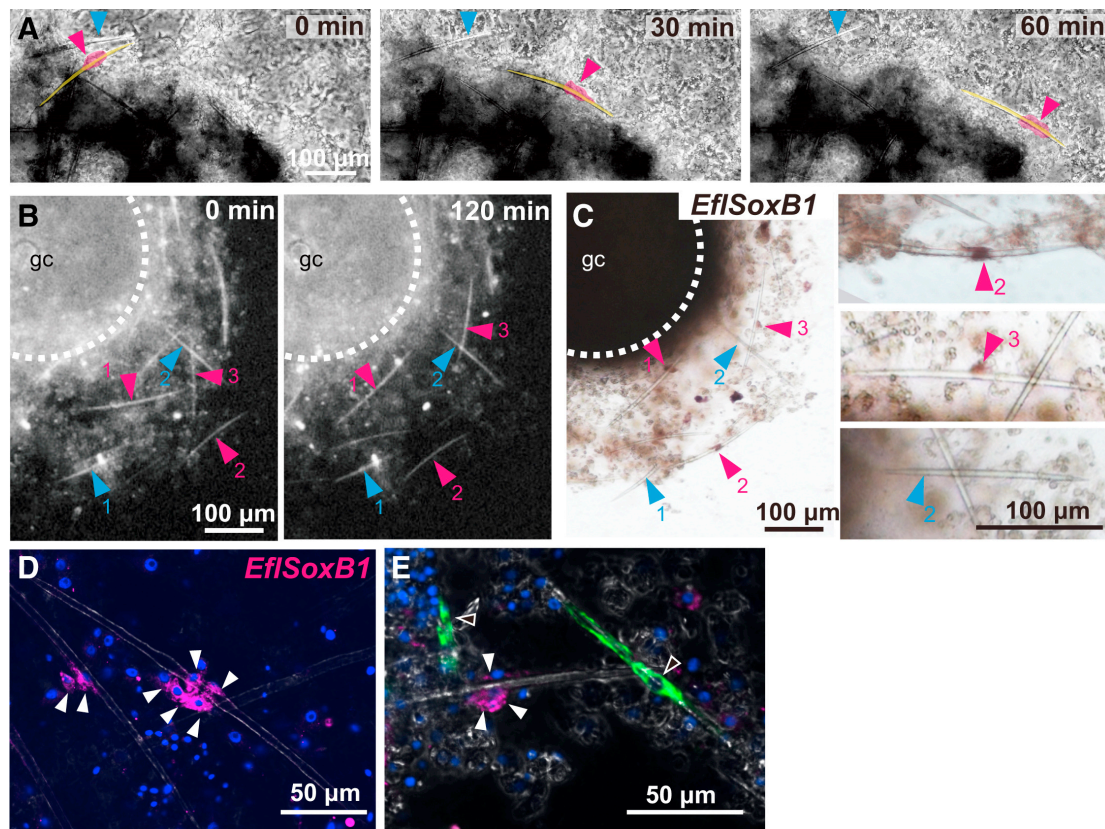


Figure 2. A Spicule Is Carried by a Group of *EflSoxB1*-Expressing Cells

(A) A moving spicule (shaded yellow; magenta arrowhead) had attached cell(s) (shaded pink), but an immobile spicule (blue arrowhead) did not. See also Movie S3. (B) Time-lapse images obtained from beneath a sponge. Numbered magenta arrowheads indicate moving spicules; numbered blue arrowheads indicate immobile spicules. (C) Subsequent detection of *EflSoxB1* mRNA expression. Moved spicules had attached *EflSoxB1*-expressing cells around their midpoint. gc, gemmule coat. Because WISH images were taken from beneath sponges, blocking of the light beam by the gemmule coat and mesohyl cells produced some artifactual brown signals. (D) Groups of *EflSoxB1*-expressing cells (white arrowheads) were attached to spicules. (E) Dual-color fluorescence in situ hybridization showed that *EflSilicateinM1*-expressing sclerocytes (green, white-bordered arrowheads) and *EflSoxB1*-expressing cells (magenta, solid white arrowheads) are different cell types (see also Figure S1). Note that the sclerocyte on the left is slightly slanted vertically rather than lying flat.

Figure 3.

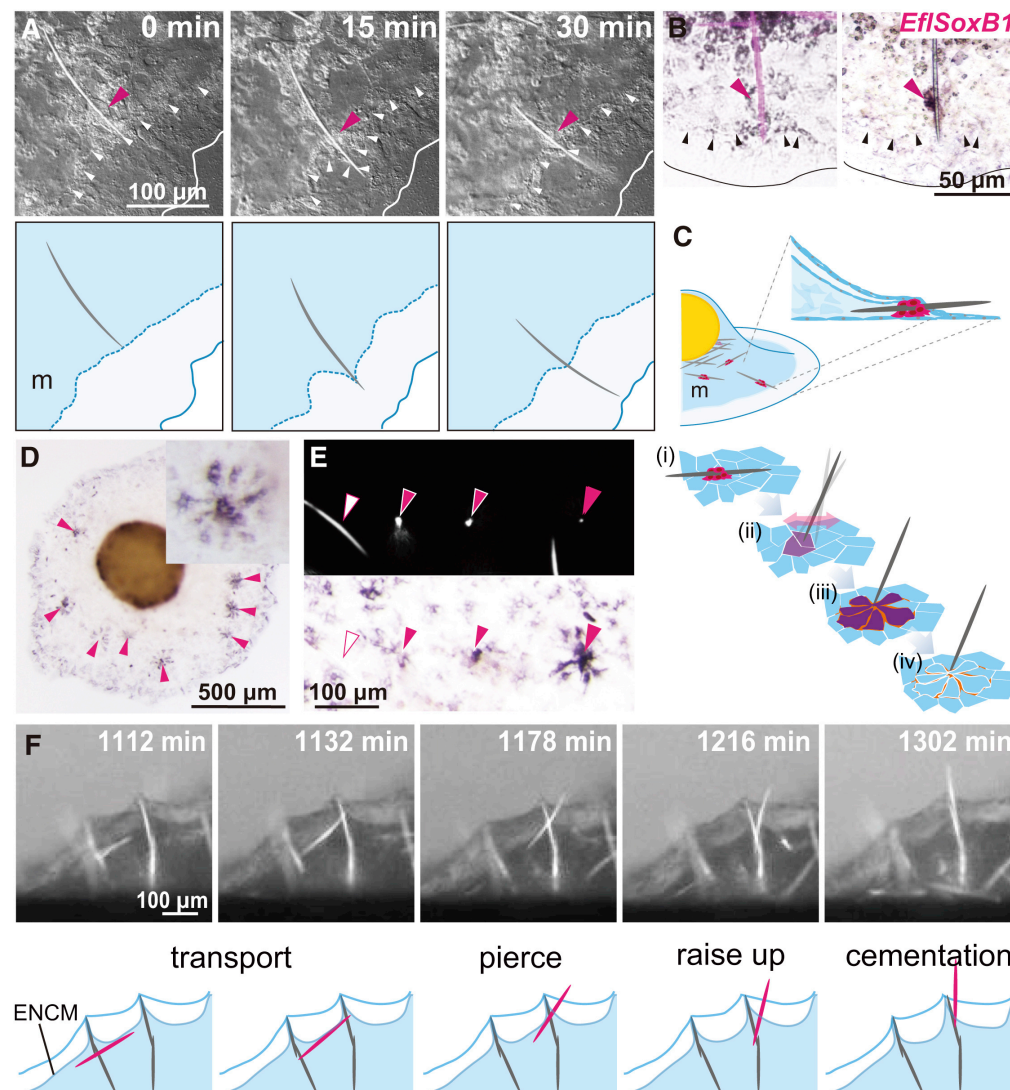


Figure 3. Process of Spicule Holding Up and Building Up

(A) Spicules pierced the outer epithelia. Upper panels show confocal time-lapse images obtained from above a sponge, and lower panels show traced illustrations. Magenta arrowhead indicates group of cells attached to a spicule. Solid white arrowheads in upper panels and dashed blue lines in lower panels indicate the edge of the mesohyl (m). White lines in upper panels and solid blue lines in lower panels indicate the rim of the sponge body. See also Movie S4. (B) Last captured image of a time-lapse video showing a spicule that started to pierce the outer epithelia (left panel) and showing the *EflSoxB1*-expressing transport cells (magenta arrowheads) (right panel). Black arrowheads indicate the edge of the mesohyl; black line indicates rim of the sponge body. See also Movie S5. (C) Schematic drawing of spicule-pierce step. (D) WISH showing that basopinacocytes arranged in rosette shape around primary spicules express *EflColS1* mRNA (magenta arrowheads; see also Figure S2). An example of more highly magnified signals in a rosette-shaped arrangement is shown in the upper right corner. (E) Left panels: last captured image of the time-lapse video (upper left panel) and subsequent detection of *EflColS1* mRNA (lower left panel). Magenta-bordered white arrowhead indicates a transported spicule near the mesohyl's edge. White-bordered magenta arrowheads indicate raised-up spicules (left: just raised up, right: 80 min after raised up). Solid magenta arrowhead indicates the spicule 75 min after the basal end became immobile. Right panel: schematic drawings showing *EflColS1* expression as a spicule becomes held up. (F) Time-lapse images obtained from the side (upper panels) with traced illustrations (lower panels). An additional spicule moves up along the inner side of the ENCM to near the top of an already held-up spicule. See also Movie S6.

Figure 4.

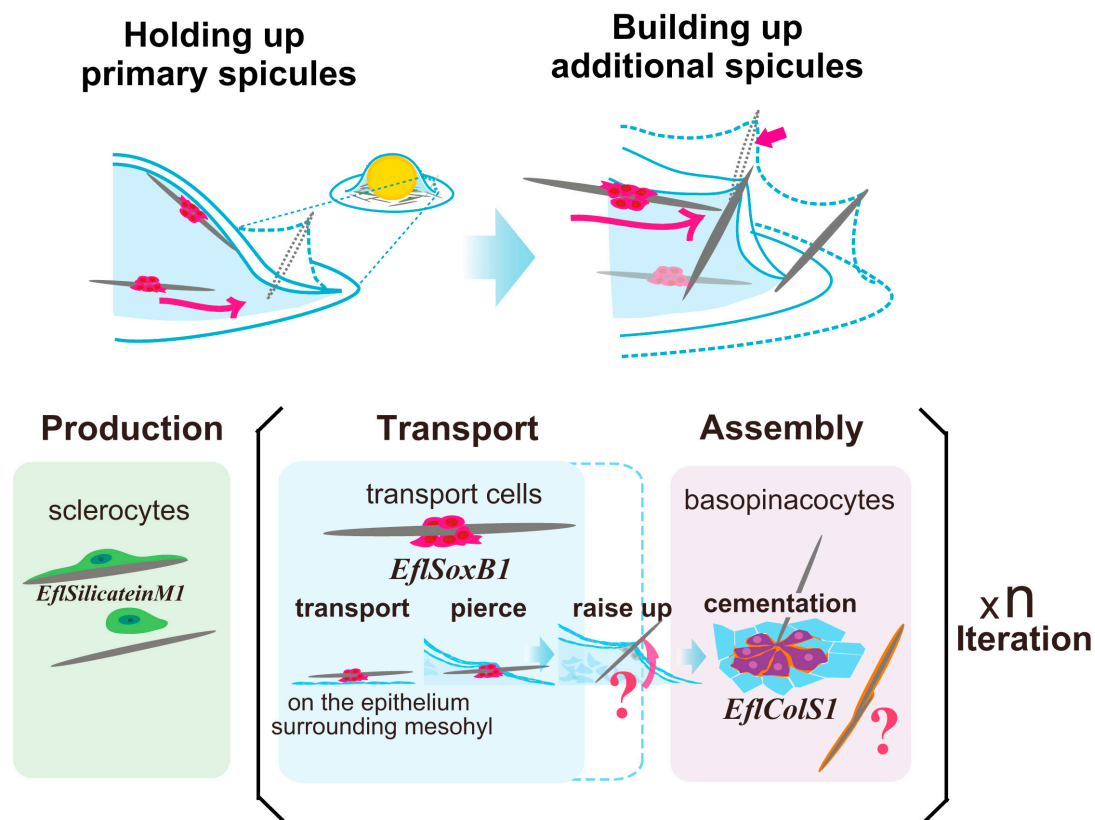


Figure 4. Spicule Transport and Iteration of Sequential Steps Construct the Skeleton of Demosponges Spicule by Spicule

Upper panel: transport cells carry spicules stochastically on the epithelium surrounding mesohyl (basopinacoderm and ENCM). Primary spicules are transported on either basopinacoderm or ENCM, but additional spicules are transported exclusively on ENCM to the top of a skeleton-constructing spicule. Lower panel: the principles of spiculous skeleton construction in demosponges revealed in this study were division of labor of spicule “production,” “transport,” and “cementation,” and the iteration of linked sequential steps of “transport,” “pierce,” “raise up,” and “cementation.” Transport cells act in “transport” and “pierce,” and possibly in “raise up”; basopinacocytes around the basal end of the raised-up spicules act in “cementation” of primary spicules. The cells that act in “cementation” of additional spicules remain to be identified in future studies.

To see Supplemental Movies, please check Current Biology 25:1-6 (2015)
[http://www.cell.com/current-biology/abstract/S0960-9822\(15\)00994-X](http://www.cell.com/current-biology/abstract/S0960-9822(15)00994-X)

Movie S1. Dynamic Movement of Spicules inside the Sponge Body, Related to Figure 1E.

Time-lapse movie showing the movement of fluorescently visualized spicules. Since Rhodamine 123 is incorporated into spicules and mitochondria, cells in the mesohyl were also visualized. First round: The moving spicules are indicated by colored arrowheads for ease of visualization of their movement. After spicules are held up, they are indicated by open arrowheads. Second round: The movement of spicules that became held up during the time-lapse recording was tracked. Time is compressed 6,000 \times .

Movie S2. Example of the Analysis of Trajectories of Spicules and the Order in which They Were Held Up, Related to Figure 1G.

Middle specimen. Z-projected time-lapse movie of specifically visualized spicules. Time is compressed 3,000 \times .

Movie S3. A Moving Spicule Has Attached Cells, Related to Figure 2A.

60 min time-lapse movie of bright-field images of a juvenile sponge taken from beneath the sponge. Spicule that was moving is shaded yellow, and attached cell(s) are shaded magenta for ease of visualization. Time is compressed 1,200 \times .

Movie S4. A Spicule Pierces through the Outer Epithelia before Its Front End Is Raised Up, Related to Figure 3A.

30 min time-lapse movie of phase-contrast confocal images of a juvenile sponge taken from above. The edge of the mesohyl can be recognized as the border between in-focus pinacoderm and out-of-focus mesohyl. Time is compressed 600 \times .

Movie S5. The Transported Spicule Starts to Pierce Outer Epithelia before Fixation for WISH, Related to Figure 3B.

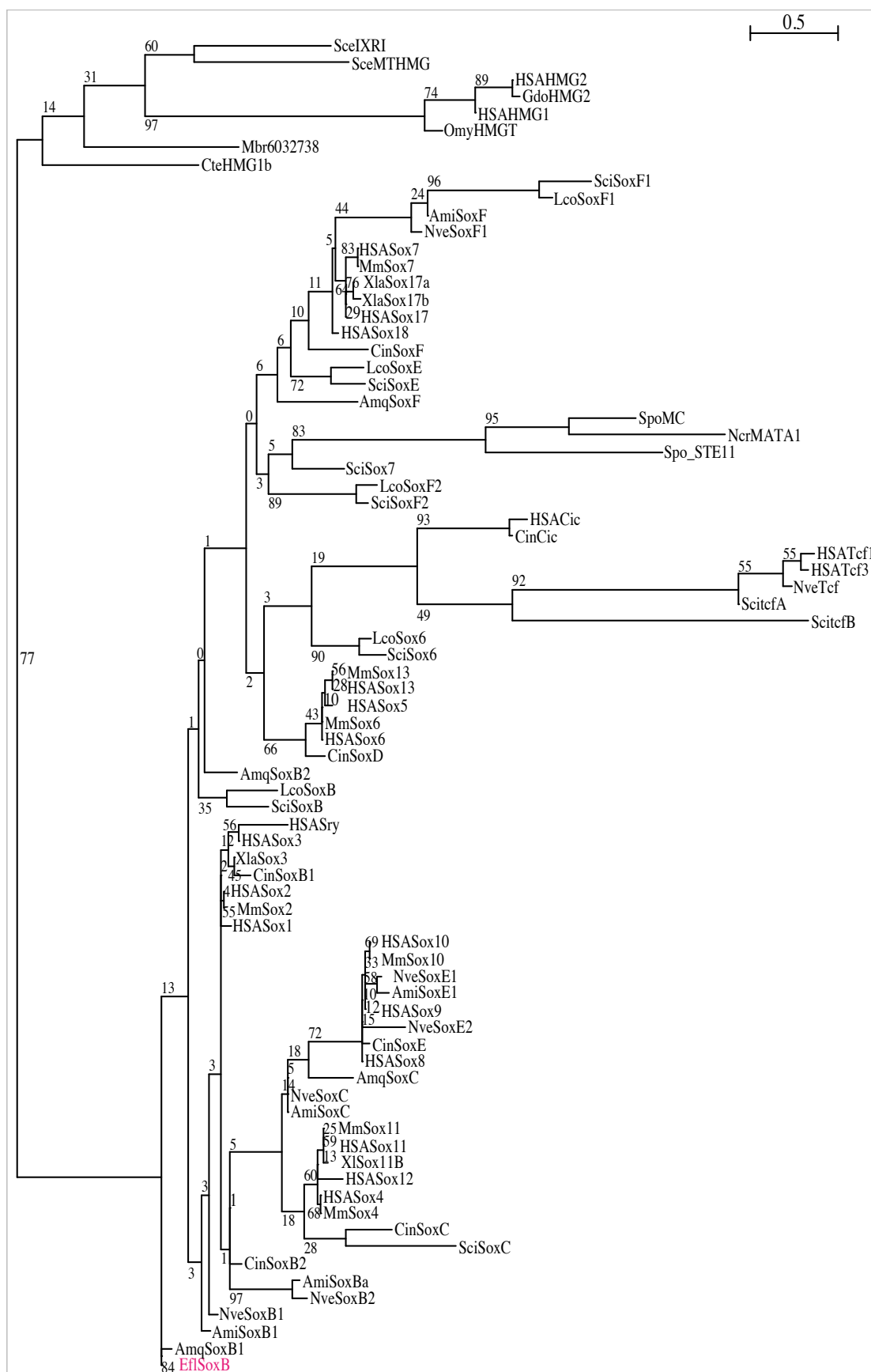
57 min time-lapse movie of merged images of bright field and the fluorescently visualized spicules showing sponge body (bright field) and spicules (shaded magenta). Time is compressed 1,800 \times .

Movie S6. Building Up the Spiculous Skeleton: View Obtained from the Side of a Juvenile Sponge, Related to Figures 1D and 3F.

24 hr time-lapse movie taken during spiculous skeleton construction. Left: the movement of spicules fluorescently visualized using 100 ng/ml TMRM (20 ng/ml TMRM during video recording). Right: bright-field image of the growing juvenile sponge from stages 2 to 5. Note that additional spicules approach already held-up spicules at an angle, and during later stages it can clearly be seen that additional spicules are carried along the inner side of the ENCM. Time is compressed 3,000 \times .

Figure S1 related to Figure 2

A



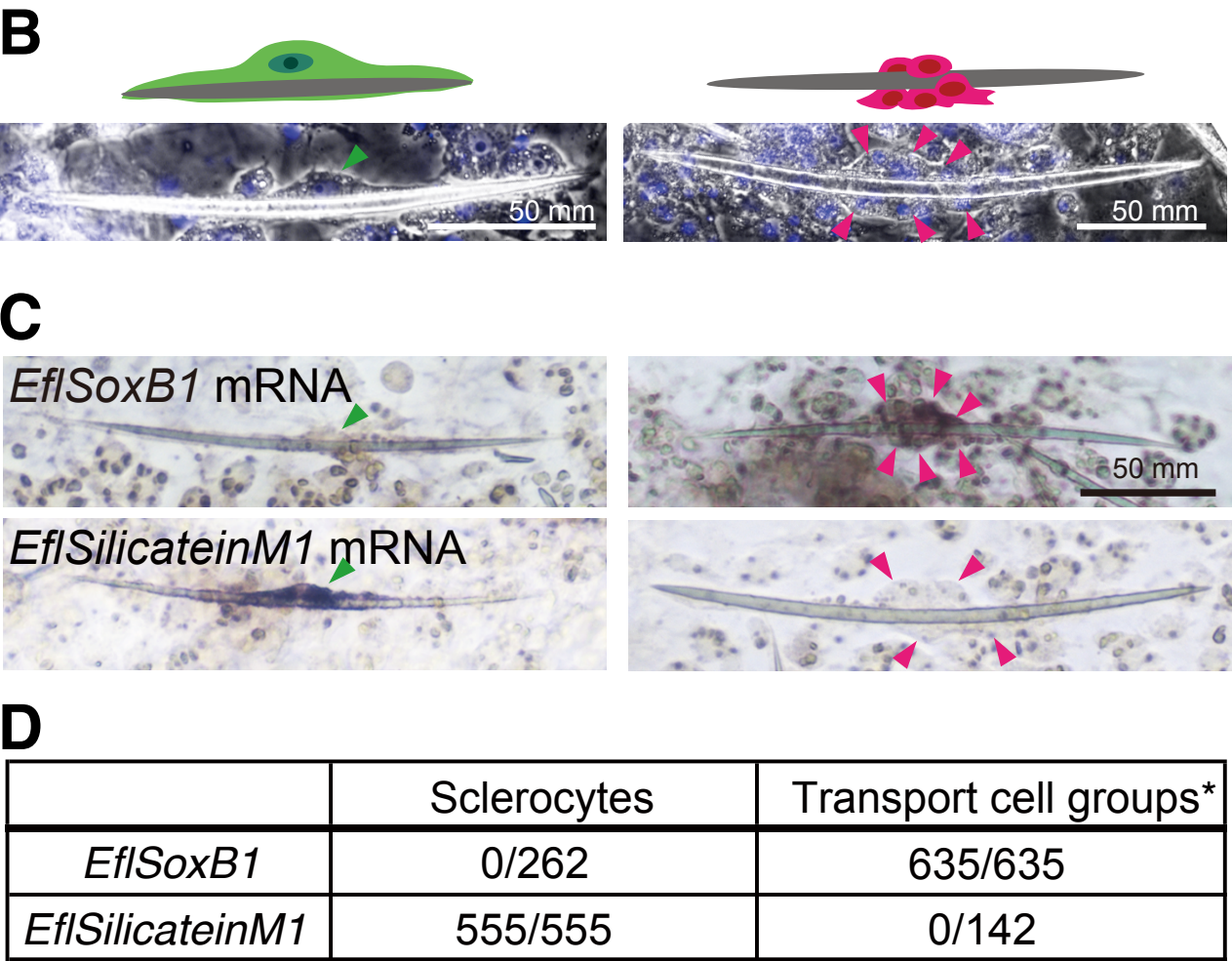


Figure S1. *EflSilicateinM1*-expressing sclerocytes and *EflSoxB1*-expressing cells are different cell types

(A) Bootstrap support values are displayed. Species names: Ami, *Acropora millepora*; Amq, *Amphimedon queenslandica*; Cin, *Ciona intestinalis*; Cte, *Chironomus tentans*; Efl, *Ephydatia fluviatilis*; Gdo, *Gallus domesticus*; Hsa, *Homo sapiens*; Lco, *Leucosolenia complicata*; Mbr, *Monoshiga brevicollis*; Mm, *Mus musculus*; Ncr, *Neurospora crassa*; Nve, *Nematostella vectensis*; Omy, *Oncorhynchus mykiss*; Sci, *Sycon ciliatum*; Spo, *Saccharomyces pombe*; Xla, *Xenopus laevis*. (B) Bright field images of a sclerocyte (left, green arrowhead) and of a group of transport cells (right, magenta arrowhead). (C) *EflSoxB1* mRNA expression is not detected in sclerocytes (upper left) but is detected in transport cells (upper right). Conversely, *EflSilicateinM1* mRNA expression is detected in sclerocytes (lower left) but not in transport cells (lower right). (D) Table: Number of counted *EflSilicateinM1*-expressing sclerocytes or *EflSoxB1*-expressing groups of cells (presumably transport cells) attached to spicules. *One group of presumptive transport cells attached to one spicule was counted as one group.

Figure S2 related to Figure 3D

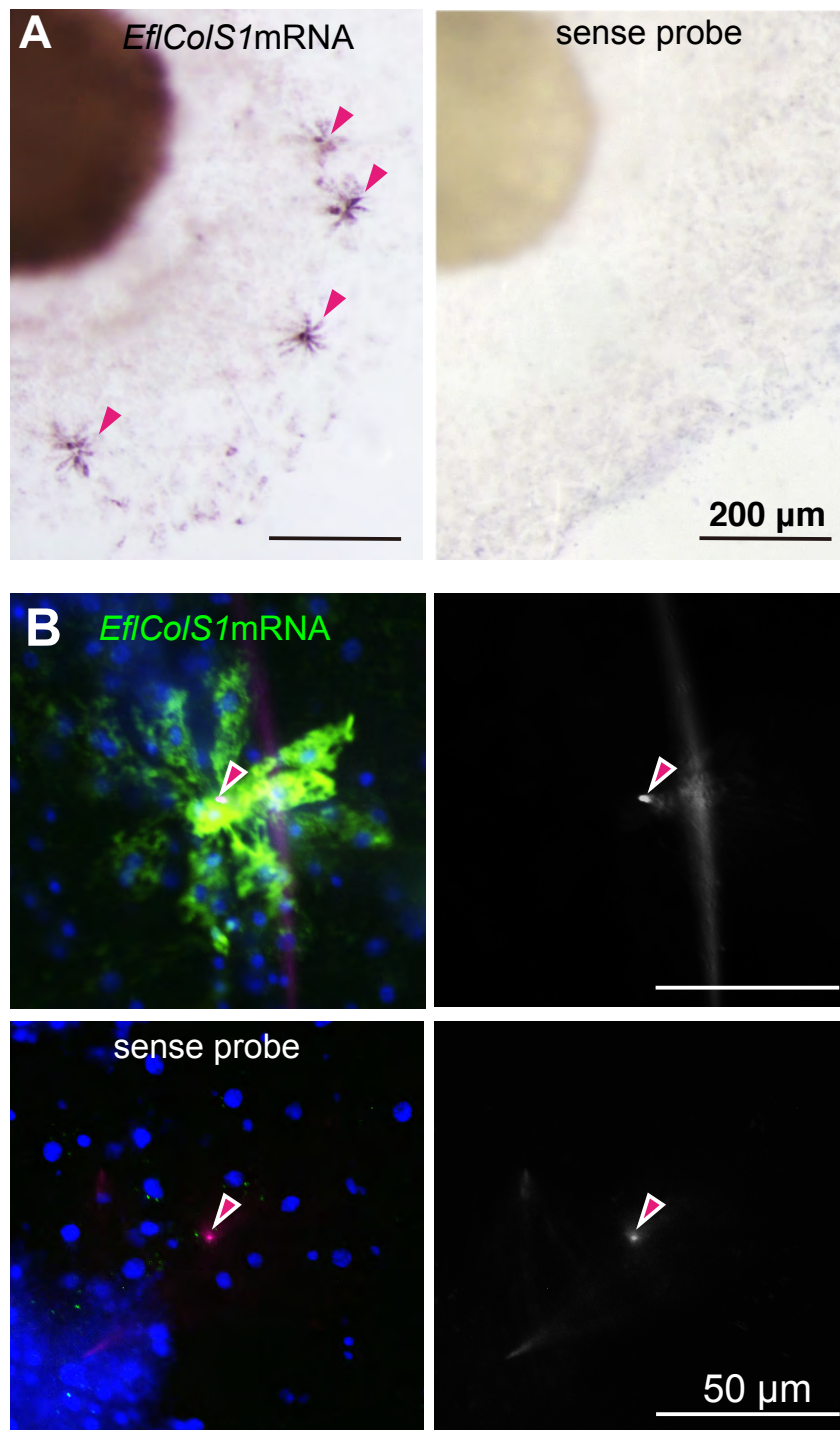


Figure S2. *EflColS1* expression around the held-up spicules.

(A) *EflColS1* mRNA expression in basopinacocytes arranged in rosette-shape around a spicule (left, magenta arrowheads) with control using sense probe of *EflColS1* (right). (B) Upper panels: *EflColS1* expression in basopinacocytes arranged in rosette-shape around fluorescently visualised held-up spicule. Lower panels: control using sense probe of *EflColS1*. Held-up spicules: white bordered magenta arrowheads.

Supplemental Experimental Procedures

Biological samples

Gemmule-bearing sponges (*E. fluviatilis*) were collected in Ibaraki and Okayama prefectures, Japan. Gemmules attached to adult sponge tissue were stored in distilled water in the dark at 4°C.

Cultivation

Gemmules were isolated and cultured as described previously[S1].

Fluorescent visualization of spicules

Rhodamine 123 (Life Technologies) or TMRM (tetramethylrhodamine methyl ester perchlorate) (Life Technologies), was used to fluorescently label spicules via deposition with SiO₂ and incorporation into siliceous spicules during their production. Juvenile sponges were cultured in M-medium with 2 mg/ml Rhodamine 123 or 20-200 ng/ml TMRM. We used TMRM (except in the experiment in Figure 1E and 2B) because TMRM specifically visualizes spicules (there is almost no TMRM incorporation in mitochondria in mesohyl cells).

Time-lapse video recording from beneath sponges

Sponges grown on glass-bottomed culture dishes (Matsunami) in M-medium with 2 mg/ml Rhodamine 123 (Life Technologies) or 200 ng/ml TMRM (Life Technologies) were used. Images were obtained using an IX-82 or IX-83 fluorescent microscopy system (Olympus), and confocal images for the time-lapse video shown in Figure 3A were obtained using a Nikon A1 confocal microscope at room temperature. For time-lapse recording with multiple Z-planes, 20 ng/ml TMRM was used. The intervals of the time-lapse recording were 10 minutes for Movies S1 (Figure 1E), 5 minutes for Movie S2 (Figure 1G), 2 minutes for Movie S3 (Figure 2A) and Movie S6 (Figure 3, 1 minute for Movie S4 (Figure 3A), and 3 minutes for Movie S5 (Figure 3B). The trajectory of one end of a moving spicule was determined by tracing back the movement of the basal end of the held-up spicule using ImageJ (NIH). Movie S2 was edited using Premier software (Adobe).

Time-lapse video recording from the side of sponges

Sponges were grown very near the edge of a microscope slide, and lateral images were obtained from the side using a mirror, with an angle of 135°. To obtain slightly stronger signals of thinner spicules in early developmental stages, sponges were grown in M-medium with 100 ng/ml TMRM, and shifted to M-medium with 20 ng/ml TMRM for time-lapse recording. Time-lapse recording was performed every 2 minutes using an IX83 (Olympus).

Isolation of *EflCollagenS1* and *EflSoxB1*

Short-chain collagen (*Ef_g5w_327G19*; *EflCollagenS1*) and SoxB homolog (*Ef_g5W_406_C02*; *EflSoxB1*) ESTs were obtained from our EST library of 5-day-old whole juvenile sponges[S1]. To obtain the full coding sequence of *EflCollagenS1*, we performed 5'RACE using *Ef_g5w_327G19* and SMARTTM according to the manufacturer's instructions

PCR primers:

5'-CGAGGCGCAACTGGCCAGAACGGTGC-3' and
5'-GACGCAGGCCAACCTGGAGAGCAAGGTC-3'.

The 5'RACE product encoded a 463-amino acid ("AA") sequence sharing 69% identity (201/209 AAs) with the sequence encoded by the partial mRNA of a short-chain collagen of *Ephydatia muelleri*[18,19], so we designated this gene *EflCollagenS1*.

Our *Ef_g5W_406_C02* (*EflSoxB1*) EST clone encoded a predicted protein of 420 AAs that included an HMG domain. Phylogenetic analysis performed using PhyML[S2] according to Fortunato *et al.*[S3] indicated that *Ef_g5W_406_C02* encoded a SoxB-type transcription factor (Figure S1A). Plasmids containing as insert *Ef_g5W_327G19* (a 1075-bp cDNA) or *Ef_g5W_406_C02-1277* (a 1277-bp cDNA produced by deleting the polyT sequence in the 3'UTR of *Ef_g5W_406_C02*) between the EcoRI and XhoI sites of pBluescript SK (+) (BD Bioscience Clontech) were used as templates to prepare cRNA probes. Both EST clones were cut with EcoRI for anti-sense cRNA probe synthesis, or with XhoI for sense cRNA probe synthesis.

Whole-mount *in situ* hybridization

Whole-mount *in situ* hybridization was performed as reported [13, S1] except that we used peroxidase-conjugated streptavidin (Perkin Elmer) instead of the peroxidase-conjugated anti-biotin antibody which we had reported using in [13].

Accession numbers, *EflSoxB1*: AB976525; *EflColS1*: AB976524.

Supplemental References

- S1. Funayama, N., Nakatsukasa, M., Hayashi, T. & Agata, K. Isolation of the choanocyte in the freshwater sponge, *Ephydatia fluviatilis* and its lineage marker, *Ef annexin*. Dev Growth Differ **47**, 243-253 (2005).
- S2. Guindon, S. et al. New algorithms and methods to estimate maximum-likelihood phylogenies: assessing the performance of PhyML 3.0. Syst biol **59**, 307-321(2010).
- S3. Fortunato, S. *et al.* Genome-wide analysis of the sox family in the calcareous sponge *Sycon ciliatum*: multiple genes with unique expression patterns. EvoDevo **3**, 14, (2012).